Persistent photoconductivity in ZnO nanorods deposited on electro-deposited seed layers of ZnO

2008 J. Phys.: Condens. Matter 20 195222

(http://iopscience.iop.org/0953-8984/20/19/195222)

J. Phys.: Condens. Matter **20** (2008) 195222 (5pp) doi:10.1088/0953-8984/20/19/195222

Persistent photoconductivity in ZnO nanorods deposited on electro-deposited seed layers of ZnO

J Nayak, J Kasuya, A Watanabe and S Nozaki

University of Electro-Communications, 1-5-1-Chofugaoka, Chofu-Shi, Tokyo-1828585, Japan

Received 5 October 2007, in final form 24 March 2008
Published 17 April 2008
Online at stacks.iop.org/JPhysCM/20/195222

Abstract
Arrays of standing nanorods of ZnO were successfully grown on indium tin oxide coated quartz substrates by an inexpensive aqueous chemical growth technique. The electrical properties of individual nanorod were investigated with the conducting tip of an atomic force microscope. The effect of ultraviolet irradiation on the conductivity of single nanorods was investigated. We observed a persistency of the photoconductivity, most probably ascribable to the oxygen vacancies in ZnO nanorods.

1. Introduction

Arrays of ZnO nanorods deserve special attention because of their applications in piezoelectric devices [1], field emission devices [2] and light emitting diodes [3]. The large surface area of the nanorods makes them suitable for gas and chemical sensor use [4]. The wide band gap (3.2 eV) and lower volume density of point defects makes ZnO nanorods efficient photocatalysts [5]. In addition, ZnO nanorods can be doped with transition elements in order to make spin polarized light sources [6]. Most of the early reports focus on the synthesis and growth mechanisms of ZnO nanorods and there have been few reports on their electrical characterization [7–11]. Physical techniques like vapor–liquid–solid [12] and chemical vapor deposition methods [13] are very common for the synthesis of ZnO nanorods. However, there are a few reports on the chemical synthesis [14] of good quality ZnO nanorods. Chemical techniques are attractive because of their simplicity and low cost. In this paper, we report the electrical characterization of chemically synthesized ZnO nanorods grown on transparent conducting oxide substrates. Our work is different from the existing reports in the following respects. We were able to successfully synthesize arrays of standing nanorods on indium tin oxide substrate. We followed a simple surfactant assisted electro-deposition technique in order to grow the ZnO seed layer, indispensable for the growth of standing nanorods, unlike in previous reports where the same seed layer was grown by complicated, expensive techniques like atomic layer deposition [15], pulsed laser deposition [16] and sputtering [17]. Using an atomic force microscope, we were able to measure the current–voltage characteristics of single, isolated nanorods. We have studied the photosensitivity of the ZnO nanorods and have observed persistency in photoconductivity.

2. Experimental details

Synthesis of ZnO nanorods on indium tin oxide (ITO) substrate involves two steps. In the first step we grew a layer of nanosized seeds of ZnO on ITO substrate by electro-deposition. In the second step, we grew ZnO nanorods on this seeded substrate by a hydrothermal deposition process. 10 ml of 0.01 M aqueous solution of $Zn(NO_3)_2{\cdot}6H_2O$ was mixed with 10 ml of 0.1 M aqueous solution of $(CH_2)_6N_4$ and the mixture was stirred for 30 min at room temperature in a 100 ml glass beaker. An electrolytic cell was designed with the above solution as the electrolyte, a platinum anode, indium tin oxide coated quartz as the cathode and a saturated calomel electrode as the reference electrode. Electrolysis was carried out at 62 °C, under potentiostatic conditions (−1.4 V) for 30 s. After the deposition, the sample was thoroughly rinsed in DI water ($\rho = 18$ MΩ cm) and dried at 50 °C for 2 h; this was followed by annealing for 20 min in oxygen atmosphere at 500 °C. The morphology of the sample was investigated using a scanning electron microscope. We observed close packed nanoseeds of ZnO on the ITO surface. During subsequent treatment, the above nanoseeds act as the nucleation centers for the ZnO nanorods. In order to grow ZnO nanorods, the seeded substrate was immersed in an aqueous solution mixture of 0.01 M $Zn(NO_3)_2{\cdot}6H_2O$ and 0.1 M $(CH_2)_6N_4$, in a sealed conical flask, and the flask was subjected to hydrothermal

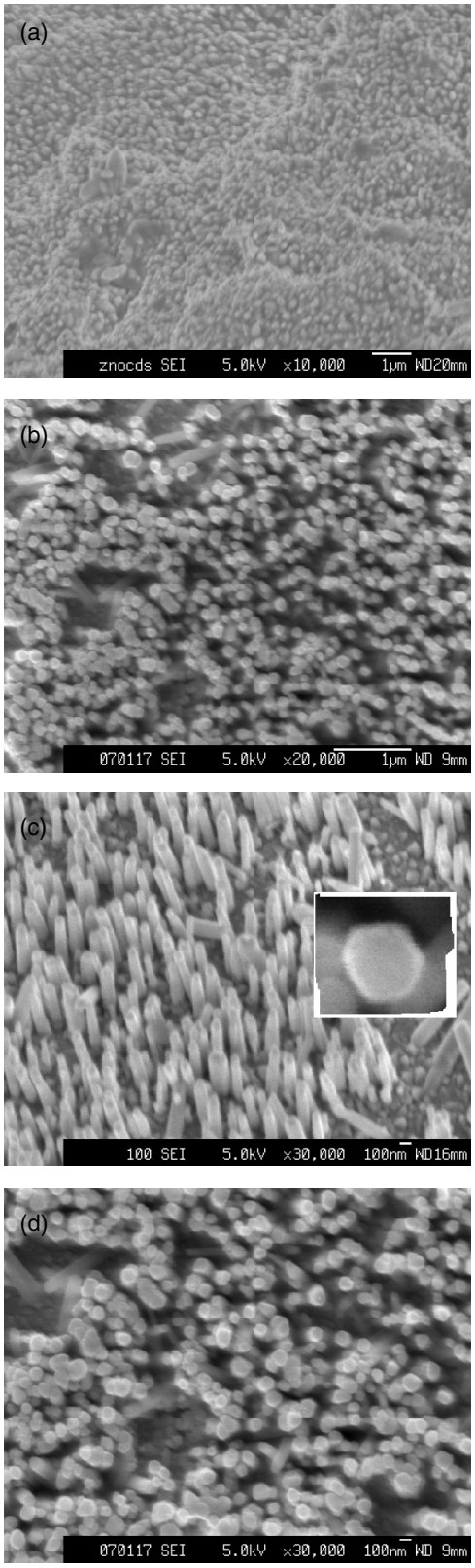

Figure 1. (a) FESEM image of an electro-deposited seed layer of ZnO, (b) normal view of the as prepared nanorods of the ZnO, deposited on the seed layer, (c) SEM image of the sample, tilted at an angle of 30° with respect to the horizontal plane (the inset shows the high magnification image of the tip of a nanorod), (d) normal view of the ZnO nanorods after annealing at 250 °C for 20 min in oxygen atmosphere.

treatment at 95 °C in a regular laboratory oven for 24 h. Then, the flask was taken out of the oven, cooled and the sample was thoroughly rinsed in DI water; this was followed by drying at about 100 °C for 2 h.

The morphology and the size of the nanorods were investigated with a JEOL JSM 3010 field emission scanning electron microscope (FESEM). In the operating condition the electron beam current was 12.5 μA and the electron energy was 5 keV. The size and the structure of the nanorods was also studied with a Philips X'pert x-ray diffractometer equipped with Cu Kα radiation ($\lambda = 1.546$ Å). The current–voltage characteristics of individual isolated nanorods of ZnO were measured with the conducting cantilever (platinum coated silicon) of a JEOL JSPM 4200 atomic force microscope.

In order to investigate the electrical properties of the individual ZnO nanorods, we followed a well-known technique pursued by early researchers [18–21]. The tip of the cantilever of an atomic force microscope was pressed on the tip of an individual nanorod of ZnO. The contact force was 2.5 μN and the cantilever was a platinum coated Si probe, specially designed for the electrical characterization of the carbon nanotubes.

3. Results and discussion

The morphologies and the dimensions of the ZnO nanorods were studied with a field emission scanning electron microscope (FESEM). Figure 1(a) shows the SEM image of a layer of homogeneous, close packed nanoseeds of ZnO electro-deposited on the indium tin oxide coated quartz substrate. This seed layer is crucial for the growth of standing nanorods [22]. Figure 1(b) shows the low magnification SEM image where one can see an array of standing nanorods of ZnO. One should notice that the orientation of the nanorods is quite good and they grow normal to the substrate surface. The nanorods have diameters ranging from 80 to 100 nm with lengths of $\sim$1 μm. Figure 1(c) shows the 30° tilted image of the nanorods where we observe them to have hexagonal cross-sections (as shown in the inset) and their tips are well separated. Figure 1(d) shows the normal view of the SEM image of ZnO nanorods annealed at 250 °C for 20 min in oxygen atmosphere. There is no such significant change in the morphology and orientation of the nanorods due to annealing. Figure 2 compares the low angle x-ray diffraction (XRD) spectra of the as deposited nanorods with those of the oxygen annealed (250 °C, 20 min) nanorods deposited on ZnO/ITO. Here, one can observe a series of peaks corresponding to (100), (002), (101) planes of hexagonal ZnO, indicating the polycrystalline nature of the ZnO nanorods. Due to annealing in the oxygen atmosphere, the crystallinity of the nanorods improves, as indicated by an increase in the intensities of the XRD peaks.

Figure 3(a) shows the AFM topographic image of the ZnO nanorods deposited on the ITO substrate where one can see spiked structure [23] having the dimension of several hundred nanometers. Figure 3(b) shows the current–voltage (I–V) characteristic of an individual ZnO nanorod, where the maximum possible value of the ratio between the forward and the reverse current is as high as 300. Such a high rectifying

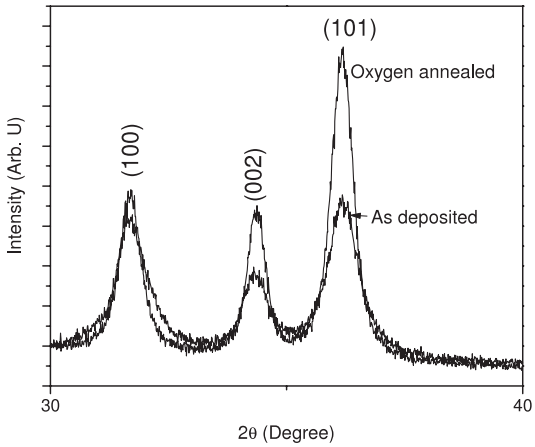

Figure 2. Low angle x-ray diffraction spectra of the as prepared and oxygen annealed (250 °C, 20 min) nanorods of ZnO deposited on ZnO/ITO.

ratio indicates a perfect Schottky junction between ZnO and Pt. The voltage plotted along the x-axis corresponds to the bias on the ITO substrate. When the ITO is negatively biased with respect to the cantilever of the AFM, the current varies exponentially with voltage. However, when the ITO is positively biased with respect to the cantilever of the AFM, the current is negligibly small and independent of the voltage. This shows that the ZnO nanorod has n-type conductivity. In order to keep the data analysis simple, we neglect the effect of the small potential barrier at the ITO/n-ZnO interface [24]. The maximum value of the electrical current is as high as 2.5 nA at −4 V, in contrast to an earlier report where the current was of the order of picoamperes [25]. This indicates a smaller ohmic resistance of our metal–semiconductor point contact because of higher contact force. The surface adsorbed species also significantly reduce the conductance of individual nanorods [26]. However, since we used a water-soluble surfactant (hexamine) and the sample was thoroughly rinsed in water after the deposition, we expect a negligible effect from the surface species.

Some researchers question the reliability of the AFM nanorod contact due to vibration of the nanorod. In this regard, we would like to mention that the time taken to record the entire current–voltage characteristic was less than one second. The cantilever was pressed against the tip of the nanorod with a contact force of 2.5 μN which is strong enough to make the effect of cantilever vibration negligible and weak enough not to break the nanorod. In order to confirm that the ITO substrate was not short-circuited with the cantilever, we measured the I–V characteristic by pressing the cantilever against the bare ITO surface (at some points on the sample where no ZnO was deposited). The corresponding I–V curve looks nearly ohmic, as shown in figure 3(c), which proves that the rectifying nature of the I–V characteristics is entirely due to the ZnO. The saturation limit for the current was set to 100 nA in our apparatus.

The UV detection characteristics of individual ZnO nanorods were investigated by illuminating the ITO/ZnO/Pt point contact junction with a UVL-56, 2.5 W cm^{-2}, 366 nm

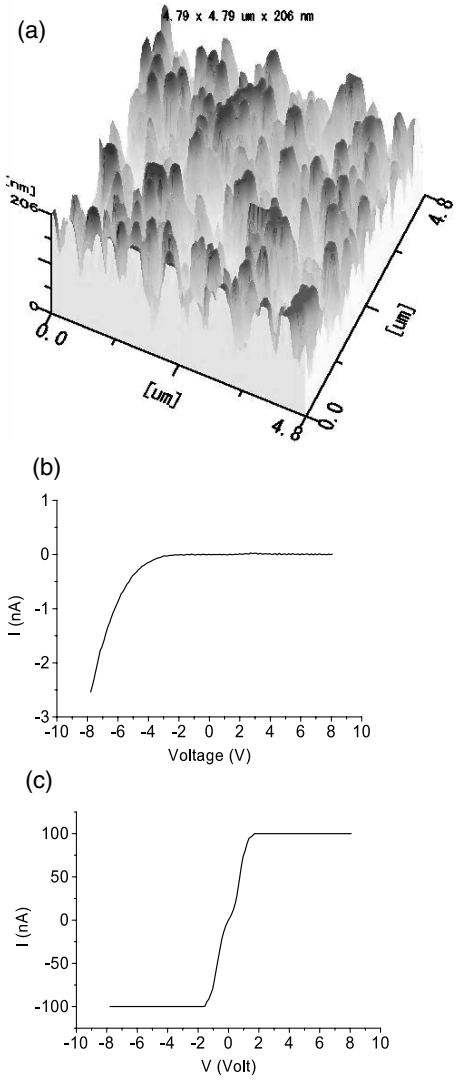

Figure 3. (a) Atomic force microscopic image of ZnO nanorods deposited on ITO, (b) current–voltage characteristics of individual nanorods, (c) current–voltage characteristics for bare ITO substrate.

UV lamp, the time of illumination was about 3 s. The current–voltage curves with and without the UV illumination are shown in figure 4. We observed a pronounced optical switching effect [27] with tenfold increase in the conductance attributed to generation of the electron–hole pairs in the ZnO nanorod due to the UV irradiation. The change in the conductance could also occur due to the process of molecular photodesorption. However, the possibility of molecular photodesorption can be easily ruled out simply because the conductivity of nanorod is supposed to decrease due to desorption of the surface molecules [28]. Again, the effect of the photodesorption is prominent under vacuum while all our measurements were carried out in ambient. Any possibility of a heating effect can be easily denied because the junction area is of the order of several hundred (nm)^2 and the illumination time was about 3 s. The sharp increase in the conductance was found to be persistent even after the UV was switched off. We recorded the I–V curves in 30 s intervals and observed that even after 6 min the current was higher than the dark current.

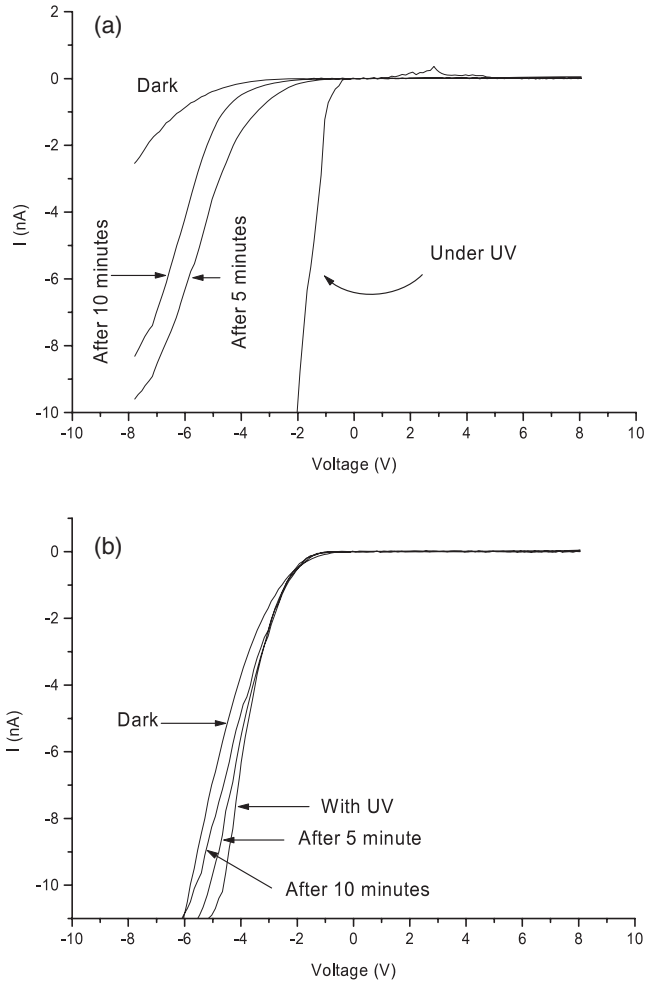

Figure 4. Current–voltage (I–V) characteristics of ZnO nanorod recorded in the dark and under UV irradiation. (a) I–V curve of as prepared ZnO nanorods; the dark curve is the same as the I–V curve in figure 3(b). (b) I–V curve of the oxygen annealed (250 °C, 20 min) ZnO nanorods.

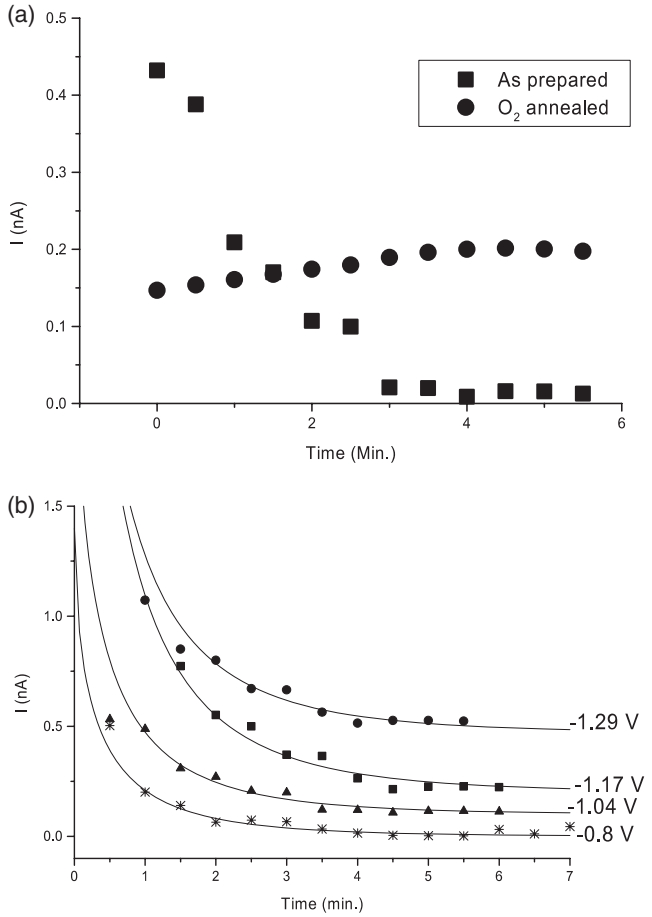

Figure 5. (a) Photocurrent decay of as prepared and oxygen annealed (250 °C, 20 min) ZnO nanorods, (b) photocurrent decay curves fitted with a stretched exponential function.

In order to check the effect of the cantilever vibration, we repeated the experiment three times and observed that the result was reproducible. Again, the I–V characteristics of bare ITO/quartz, separately recorded with and without the UV irradiation, had ohmic character with no photoeffect. The next section of the paper explains the observed persistency in the photoconductivity.

In order to explain the observed persistency in the photocurrent, the ZnO nanorods were annealed in oxygen atmosphere at 250 °C for 20 min. The current–voltage characteristic of the annealed sample is displayed in figure 4(b) where one can observe a very small persistency in the photocurrent. Figure 5(a) compares the time dependent photocurrent decay of as prepared sample with that of the annealed sample. One can notice that the decay curve for the annealed sample is completely flat, showing very weak persistency of the photoconductivity. Looking at the above result, we suggest that the persistency in the photocurrent could be attributed to trapping of the photogenerated charge carriers in the point defects like oxygen vacancies [29] in the ZnO nanorods. Due to annealing in the oxygen atmosphere, the volume density of the oxygen vacancies decreases on account of incorporation of the oxygen atoms into the ZnO lattice [30]. Therefore we observe, under UV illumination, a very small change in the conductivity and again, after the UV was switched off, the conductivity approaches the dark value very fast, in this way, showing negligible persistency in the photoeffect. The above explanation is just a preliminary idea. Right now we are not aware of the exact reason behind the observation of persistency in the photocurrent and experiments are in progress to explore the same.

One important feature of our current–voltage measurement result is the observation of a small enhancement of the dark conductivity of the ZnO nanorod on account of annealing in oxygen atmosphere as shown in figure 5(a). Similar enhancement in the conductivity of the nanorod of ZnO due to oxygen annealing was observed by Zhao *et al* who interpreted it as being due to the passivation of the surface oxygen vacancies [31]. Again, the annealing causes an improvement in the crystallinity of the ZnO nanorods as seen in the XRD spectra, which could be responsible for the increase in the conductivity. Moreover, since we prepared our ZnO nanorods in alkaline environments, there could be ultrasmall $Zn(OH)_2$ particles dispersed in the ZnO matrix which are responsible for scattering

of the conduction band electrons. Due to the annealing, the decrease in the content of $Zn(OH)_2$ improves the conductivity [32].

It is well known that the quantitative analysis of the photocurrent decay process involves the fitting of the decay curve with stretched exponential functions in order to calculate the decay time constant and the decay exponent [33–36]. As shown in figure 5(b), the decay curves were fitted with a stretched exponential function of the following form [37]:

$$I = I_0 + C_1 \exp[-(t/\tau)^{\alpha}], \quad (1)$$

where I_0 is the steady state photocurrent, t is the time, C_1 is the scaling constant, τ is the decay time constant and α is the decay exponent. The values of τ and α were found to be 200 s and 0.58 with an error of 0.5%, respectively. A smaller value of the decay time constant compared to that reported earlier [38] indicates a lower density of oxygen vacancies in our ZnO nanorod.

4. Conclusion

It was possible to grow a layer of nanoseeds of ZnO on transparent conducting oxide substrate by an inexpensive, surfactant assisted electro-deposition technique. The above seed layer played the key role in the growth of aligned nanorods of ZnO normal to the substrate surface. The ZnO nanorods were observed to work as efficient UV detectors, as indicated by a significant enhancement of their conductivity on account of the UV irradiation. The photoconductivity persists for 6 min because of trapping of the charge carriers by oxygen vacancies, acting as deep traps.

References

[1] Wang X, Sung J, Liu J and Wang Z L 2007 *Science* **316** 102–5
[2] Li L M, Du Z F, Li C C, Zhang J and Wang T H 2007 *Nanotechnology* **18** 355606
[3] Park B W and Yi G C 2004 *Adv. Mater.* **16** 87–90
[4] Wang H T, Kang B S and Ren F 2005 *Appl. Phys. Lett.* **86** 243503–5
[5] Poulios I, Makri D and Prohaska X 1999 *Global Nest The Int. J.* **1** 55–62
[6] Norton D P, Pearton S J and Hebard A F 2003 *Appl. Phys. Lett.* **82** 239–41
[7] Li Q H, Wan Q, Liang Y X and Wang T H 2004 *Appl. Phys. Lett.* **84** 4556–8
[8] Keem K, Kim H, Kim G T, Lee J S and Kim S 2004 *Appl. Phys. Lett.* **84** 4376–8
[9] Kind B H, Yan H, Messer B and Law M 2002 *Adv. Mater.* **14** 158–60
[10] Liu C H, Liu W C, Au F C K, Ding J X and Lee S T 2003 *Appl. Phys. Lett.* **83** 3168–70
[11] Park W I, Yi G C, Kim J W and Park S M 2003 *Appl. Phys. Lett.* **82** 4358–60
[12] Huang M H, Mao S and Feick H 2001 *Science* **292** 1897–9
[13] Cong G W, Wei H Y, Zhang P F, Peng W Q, Wu J J and Wang Z G 2005 *Appl. Phys. Lett.* **87** 231903–5
[14] Vayssieres B L 2003 *Adv. Mater.* **15** 464–6
[15] Li Q, Kumar V, Li Y, Zhang H, Marks T J and Chang R P H 2005 *Chem. Mater.* **17** 1001–6
[16] Sun B Y, Fuge G M, Fox N A, Riley D J and Ashfold M N R 2005 *Adv. Mater.* **17** 2477–81
[17] Song J and Lim S 2007 *J. Phys. Chem.* C **111** 596–600
[18] Ghosh R and Basak D 2007 *Appl. Phys. Lett.* **90** 243106
[19] Schlenker E, Bakin A, Postels B, Mofor A C, Wehmann H H, Wiemann T, Hinze P and Waag A 2007 *Phys. Status Solidi* b **244** 1473–7
[20] Park W I, Yi G-C, Kim J M and Park S M 2003 *Appl. Phys. Lett.* **82** 4358–60
[21] Luo J, Zhu J, Huang Z and Zhang L 2007 *Appl. Phys. Lett.* **90** 033114 (3)
[22] Guo M, Diao P and Cai S 2005 *J. Solid State Chem.* **178** 1864–73
[23] Yang B Y J L, An S J, Park W I, Yi G C and Choi W 2004 *Adv. Mater.* **16** 1661–4
[24] Zugang L, Weiming Z, Rongbin J and Bin F 1996 *J. Phys.: Condens. Matter* **8** 3221–8
[25] Fan Z, Dutta D, Chien C J, Chen H Y and Brown E C 2006 *Appl. Phys. Lett.* **89** 213110–2
[26] Fan Z Y, Wang D W and Chang P C 2004 *Appl. Phys. Lett.* **85** 5923–5
[27] Park J Y, Yun Y S, Hong Y S, Oh H, Kim J J and Kim S S 2005 *Appl. Phys. Lett.* **87** 123108
[28] Chen R J, Franklin N R, Kong J, Cao J, Tumbler T W, Zhang Y and Dai H 2001 *Appl. Phys. Lett.* **79** 2258–60
[29] Zhang S B, Wie S H and Zunger A 2001 *Phys. Rev.* B **63** 075205
[30] Zhang D H, Xue Z Y and Wang Q P 2002 *J. Phys. D: Appl. Phys.* **35** 2837–40
[31] Zhao Q, Xu X Y, Sung X F, Zhang X Z and Yu D P 2006 *Appl. Phys. Lett.* **88** 033102
[32] Kobayashi S, Oshima K, Sasaki T, Tsuboi N and Kaneko F 2005 *Japan. J. Appl. Phys.* **44** 1372–5
[33] Vardeny Z, O'Connor P, Ray S and Tauc J 1980 *Phys. Rev. Lett.* **44** 1267–9
[34] Lopatiuk O and Chernyak L 2005 *Appl. Phys. Lett.* **87** 214110–2
[35] Dissanayake A, Elahi M, Jiang H X and Lim J Y 1992 *Phys. Rev.* B **45** 13996–4004
[36] Li J Z, Lin J Y, Jiang H X, Salvador A, Botchkarev A and Morkoc H 1996 *Appl. Phys. Lett.* **69** 1474–6
[37] Poti B, Passaseo A, Lomascolo M, Cingolani R and De Vittori M 2004 *Appl. Phys. Lett.* **85** 6083–5
[38] Reemts J and Kittel A 2007 *J. Appl. Phys.* **101** 013709